Docking and molecular dynamics simulation of the Azurin–Cytochrome c551 electron transfer complex

Anna Rita Bizzarri[1]*, Elena Brunori[1], Beatrice Bonanni[1,2] and Salvatore Cannistraro[1]

[1]Biophysics and Nanoscience Centre, CNISM, Faculty of Science, Università della Tuscia, Largo dell'Università, I-01100 Viterbo, Italy
[2]CNR-INFM, Dipartimento di Scienze Ambientali, Università della Tuscia, Largo dell'Università, I-01100 Viterbo, Italy

We coupled protein–protein docking procedure with molecular dynamics (MD) simulation to investigate the electron transfer (ET) complex Azurin–Cytochrome c551 whose transient character makes difficult a direct experimental investigation. The ensemble of complexes generated by the docking algorithm are filtered according to both the distance between the metal ions in the redox centres of the two proteins and to the involvement of suitable residues at the interface. The resulting best complex (BC) is characterized by a distance of 1.59 nm and involves Val23 and Ile59 of Cytochrome c551. The ET properties have been evaluated in the framework of the Pathways model and compared with experimental data. A 60 ns long MD simulation, carried on at full hydration, evidenced that the two protein molecules retain their mutual spatial positions upon forming the complex. An analysis of the ET properties of the complex, monitored at regular time intervals, has revealed that several different ET paths are possible, with the occasional intervening of water molecules. Furthermore, the temporal evolution of the geometric distance between the two redox centres is characterized by very fast fluctuations around an average value of 1.6 nm, with periodic jumps at 2 nm with a frequency of about 70 MHz. Such a behaviour is discussed in connection with a nonlinear dynamics of protein systems and its possible implications in the ET process are explored. Copyright © 2007 John Wiley & Sons, Ltd.

Keywords: docking; molecular dynamics simulation; electron transfer; metalloproteins

INTRODUCTION

Electron transfer (ET) proteins play a key role in many biological processes, such as photosynthesis and respiration (Marcus and Sutin, 1985). Chains of redox enzymes containing metal ions, are arranged in order to assist electron flow and generate charge separation which represents the first step in the energy-capture process (Bendall, 1996; Bizzarri and Cannistraro, 2005). An electron moves from a donor (D) to an acceptor (A), flowing down a gradient of potential through a chain of redox centres which may be separated by a relatively large distance (1–2 nm or even more) (Marcus and Sutin, 1985). Recently, the ET capabilities of biomolecules have been combined with processing power of microelectronics to create hybrid systems for the realization of biosensors (Willner and Katz, 2000; Marvin and Hellinga, 2001; Andolfi and Cannistraro, 2005; Bonanni *et al.*, 2005).

The formation of ET complexes is envisaged to take place in two stages: first D and A form a so-called encounter complex which may be constituted by an ensemble of energetically similar complexes of the two partners (Crowley and Ubbink, 2003). Typically, the encounter complex is guided by long-range electrostatic forces (Gabdoulline and Wade, 2001). In the second stage, proteins undergo rotational and vibrational motions giving rise to a more specific reactive complex which enables the ET event (Northrup and Erickson, 1992; Ullmann *et al.*, 1997). The reactive complex might therefore, comprise, instead of a single structure, of a group of alternative structures (Liang *et al.*, 2004). The association specificity of a protein–protein complex depends on the structural properties of interfaces which should be geometrically and chemically complementary: a good matching of hydrophobic surface areas, the formation of hydrogen bonds, etc. Since high-turn over conditions are necessary to sustain a continuous electron current, ET complexes have a transient character, i.e. protein partners continuously assemble and dissociate (Nooren and Thornton, 2003), therefore, they are not easily amenable to direct experimental analysis (Mathews *et al.*, 2000; Crowley and Ubbink, 2003; Prudêncio and Ubbink, 2004).

In this respect, computational docking procedures, which provide a valuable tool in the prediction of protein–protein interactions (Janin and Rodier, 1995), could help in the study of ET complexes. The docking algorithms start from independently determined coordinates of the component proteins, performing a search of possible conformations for the complex, based on different criteria (geometric and energy interaction, etc.) (see Chothia and Janin, 1975; Jones and Thornton, 1996; Smith and Sternberg, 2002; Vajda and

Camacho, 2004). A two-stage approach is generally adopted. In the initial stage, the two proteins are treated as rigid bodies and the rotational and translational degrees of freedom are fully explored with scoring functions reflecting conformational changes. In the successive stage, the structures obtained in the initial stage are refined and re-ranked by using additional criteria that take into account experimental data; e.g. residues involved or excluded in the interaction, the molecular flexibility, etc. Nonetheless, the docking complex determination for ET protein partners might yield controversial results since their inherent transient character requires a subtle balance among quantities which should guarantee stability, efficiency and, at the same time, a high turn over.

Here, we are interested in the complex between Azurin (AZ), an electron carrier in the respiratory chain of *Pseudomonas Aeruginosa* (Solomon *et al.*, 1992; Guzzi *et al.*, 1997; Arcangeli *et al.*, 1999; Farver *et al.*, 1999; Paciaroni *et al.*, 1999; Webb and Loppnow, 1999), and the heme-protein Cytochrome c551 (C551), involved in the denitrification process (Silvestrini *et al.*, 1982; Gray and Winkler, 1996; Ceruso *et al.*, 2003). *In vitro* studies have shown that AZ exchanges electrons with C551 (Cutruzzolà *et al.*, 2002). Furthermore, atomic force spectroscopy experiments have probed the specificity and the biorecognition between these two protein partners, also allowing us to evaluate the protein–protein interaction forces and the k_{off} rate (Bonanni *et al.*, 2005; Bonanni *et al.*, 2006).

However, since this complex is not accessible to crystallographic investigation, most likely due to its limited lifetime, its real spatial arrangement is still missing.

With the aim to investigate the relative spatial positions of the two proteins in the complex, their contact regions and the ET rate and path, we have applied a protein–protein docking procedure integrated with a molecular dynamics (MD) simulation. For docking, we have used GRAMM, a molecular recognition procedure that attempts to find the best steric fit between the two molecules, by taking into account hydrophobic interactions (Vakser and Aflalo, 1994; Vakser *et al.*, 1999).

The set of favourable complexes, extracted by the docking, has been first analyzed in terms of (i) the distance between the two redox centres (more specifically the metal-to-metal distance); (ii) the contact area between the two proteins; (iii) the ratio of polar to nonpolar amino acids at the interface and (iv) the number of newly formed H-bonds. Successively, we have selected as the best complex (BC) the one having the shortest metal-to-metal distance, and involving at the interface the residues Val23 and Ile59 of C551, according to Cutruzzolà *et al.* 2002. Together with the structural properties of this complex, we have analyzed the ET properties by also comparing them with the available experimental data (Cutruzzolà *et al.*, 2002).

An MD simulation, carried out for 60 ns at full hydration, of the BC has allowed us to put into evidence that the two proteins substantially maintain their initial relative arrangement upon forming the complex. An analysis of the complex structures, sampled during the dynamics, has revealed that the ET properties change in time with respect to involvement of different residues and the occasional participation of a few water molecules, suggesting a dynamically assisted ET process. Furthermore, the metal-to-metal distance monitored as a function of time, is characterized by fast fluctuations around a value of 1.6 nm, with periodic jumps to a value of 2 nm about every 15 ns; such a behaviour, indicative of nonlinear dynamics, has suggested some implications to the ET properties of the complex.

COMPUTATIONAL METHODS

Structures of AZ and C551

The X-ray structure of AZ was obtained from the PDB (4AZU entry) (Nar *et al.*, 1991). The structure of AZ, a blue copper protein (14.5 kDa) of 128 amino acids, consists of eight β-strands forming two β-sheets in a greek-key motif. The redox site is coordinated by three ligands: N^δ of His46, N^δ of His117 and S^γ of Cys112, forming an equatorial plane around the copper. Moreover, two weaker ligands are present: S^δ of Met121 and the carbonyl group of Gly45. The copper ligand His117 protrudes through the protein surface and is surrounded by a cluster of hydrophobic residues (Met13, Leu49, Val43, Met44, Met64, Phe114, Pro115, Gly116, Ala119 and Leu120), known as the 'hydrophobic patch' (van de Kamp *et al.*, 1990). Opposite to the copper site, a disulphide bridge is located.

The X-ray structure of C551 was obtained from the PDB (451C entry) (Matsuura *et al.*, 1982). C551 is a heme-protein of class I cytochrome *c* (9.1 kDa), consisting of 82 amino acids organized in four α-helices. The heme active site is coordinated to three strong ligands, sulphurs of Cys12 and of Cys15, one nitrogen of His16 and to the axial sulphur of Met61. The heme is located slightly off-centre, with one edge exposed to the solvent. Such an exposed side, located at the border of a hydrophobic patch (Gly11, Val13, Ala14, Met22, Val23, Pro58, Ile59, Pro60, Pro62, Pro63 and Ala 65) and close to a region rich in positively charged residues, was thought to be involved in docking and ET processes with the redox partners, that possess a negatively charged surface patch (Cutruzzolà *et al.*, 2002).

Docking procedure

GRAMM is a protein–protein docking algorithm based on molecular recognition algorithms developed by Katchalski-Katzir *et al.* (1992) estimating surface complementary between the two proteins treated as rigid bodies (Vakser and Aflalo, 1994; Vakser *et al.*, 1999; Tovchigrechko *et al.*, 2002; Jiang *et al.*, 2003). The GRAMM algorithm selects complexes on the basis that protein–protein interfaces are more hydrophobic than the rest of the protein surface (Jones and Thornton, 1996). Such an algorithm, which can be applied both at low and high resolution (Tovchigrechko *et al.*, 2002; Jiang *et al.*, 2003), provides a sorted list of energy scores indicating the extent of geometric match between the surfaces of the molecules at different relative positions. The atomic coordinates of each protein were first projected, for a digital representation, on a three-dimensional grid of $N \times N \times N$ points where they were represented by discrete functions to distinguish among the inside, outside and on the surface of molecules; the

surface being represented as a boundary layer of finite width between the interior and the external part of the molecule. Small positive numbers were assigned to the surface of the bigger protein (AZ), while large negative numbers were assigned to its interior to penalize for penetration in the core of the protein. The AZ (receptor) was held fixed and C551 (ligand) was translated and rotated around the receptor searching through all the conformational space in six dimensions. For each configuration, the correlation function, evaluating the degree of the geometric match between the two molecules, was calculated using Fast Fourier Transform (FFT). We applied GRAMM high resolution generic mode, with the following docking parameters: grid step 1.7 Å, grid size 64 Å, the energy score for repulsion 30, the energy score for attraction −1 and intervals of rotation of ligand around to receptor 10°. The 100 structures yielding the best (highest) energy scores, among 1000 of outcomes, were selected and considered for further analysis.

MD simulation

The MD simulations were carried out by using the GROMACS 3.2 package (Berendsen *et al.*, 1995; Lindahl *et al.*, 2001), including the potential force field Gromos96 (van Gunsteren *et al.*, 1996). The initial coordinates of the AZ–C551 complex were taken from the results of docking procedure (see the Results and Discussion Section). The copper ion of AZ was covalently bound to three ligands: two nitrogens from His46 and His117, respectively, one sulphur from Cys112, while the much weaker interactions of copper with the sulphur from Met121 and carbonyl oxygen from Gly45 were treated by a nonbonded approach (Arcangeli *et al.*, 1999). The partial charges for the copper and its ligand residues were modified according to those reported in (Swart, 2002); the copper charge having been fixed to 0.33e. The heme group of C551 was covalently bound to three ligands: two sulphures from Cys12 and Cys15, respectively, and one nitrogen from His16. Atomic charges, all angles and bonds involving the heme site, were fixed as the parameters present in Gromos96. The charge of iron was set to 0.40e. All ionizable residues of both proteins, with the exception of copper and heme ligands, were assumed to be in the ionization state corresponding to pH 7.0.

The complex was centred in a fixed-volume rectangular box with dimension 7.7 nm × 4.8 nm × 6.0 nm, filled by SPC/E water molecules (Berendsen *et al.*, 1997). Solvent molecules whose distance from any atom of the solute molecules was less than 0.23 nm, were deleted. To ensure the neutrality of the system, five water molecules were replaced by five chlorine counterions. The final hydrated system contains 6253 water molecules resulting in a hydration level of 3.8 g of water per g of protein, corresponding to full hydration. The LINCS algorithm was used to constrain the bond lengths (Hess *et al.*, 1996). Short-range electrostatic and van der Waals forces, with a cutoff radius of 0.9 nm, were calculated for all pairs of a neighbour list, updated every 10 steps, with nearest-image distances higher than 1 nm. Electrostatic interactions were calculated by the Particle Mesh Ewald (PME) method (Darden *et al.*, 1993; Kholmurodov *et al.*, 2000). For the calculation of the reciprocal sum, the charges were assigned to a grid in real space with a lattice constant of 0.12 nm using fourth order cubic spline interpolation.

After the energy minimization, the temperature, initially set at 50 K, was increased up to 300 K in 500 ps by steps of 5 K. Then, the MD simulation was carried out, by applying periodic boundary conditions, with a step size of 2 fs, at constant temperature and volume (NVT ensemble), by using the Nosè-Hoover thermostat with a time constant of 0.1 ps (Nosé, 1984). The run consists of 60 ns by collecting data every 50 fs for analysis. For comparison, MD simulations of both isolated AZ and C551 were carried out at the same hydration level of the complex. The initial coordinates of AZ and C551 were taken from the crystallographic structures (see above).

RESULTS AND DISCUSSION

Analysis of docking complexes

Docking procedures are able to sort out a number of suitable complexes, ordered by their energy score, also including false positive matches. Hence, docking outcomes should be refined by additional criteria in order to single out near-native structures. Among the different sorted AZ–C551 complexes, we have retained the first 100 complexes with the highest energy scores for further analysis. A preliminary analysis by visual inspection of the sorted complexes has revealed that the two partners assume different relative positions in the complex.

Most of these sorted complexes involve the hydrophobic patches of both the proteins at the protein–protein interface. This finds a correspondence with the experimental evidence that these regions play a major role in the formation of the complex and in the successive ET process (Cutruzzolà *et al.*, 2002). We note in passing that the S–S bridge of AZ is not involved in the protein–protein interface for the largest part of sorted complexes. This fact can be exploited in hybrid nanodevices to anchor AZ to gold through its S–S bridge by maintaining the opposite reactive region, available for interactions with ET partners (Bizzarri *et al.*, 2005; Bonanni *et al.*, 2005).

For each of the sorted docking complexes, we have analyzed: (i) the distance between the two redox centres; (ii) the Interface Accessible Surface Area (I-ASA); (iii) the ratio of the polar to nonpolar amino acids at the interface and (iv) the number of additional H-bonds.

The distance between the two redox centres constitutes a crucial parameter for the ET efficiency of the resulting complex (Marcus and Sutin, 1985; Moser *et al.*, 1992). Actually, an interprotein ET process typically occurs over distances of 1–2 nm, and it may be mediated by the intervening medium between D and A. In short–distance reactions, electronic orbitals of D and A are directly overlapped, whereas in long distance reactions, this coupling is indirect because of sequential overlaps of the atomic D and A orbitals of the intervening medium (Bendall, 1996). Even if different models have been proposed to describe the ET process, a decrease in ET rates for longer D–A distances, is generally ascertained (Beratan *et al.*, 1987; Moser *et al.*, 1992). We have evaluated the distance between the two redox centres by monitoring the geometric distance between
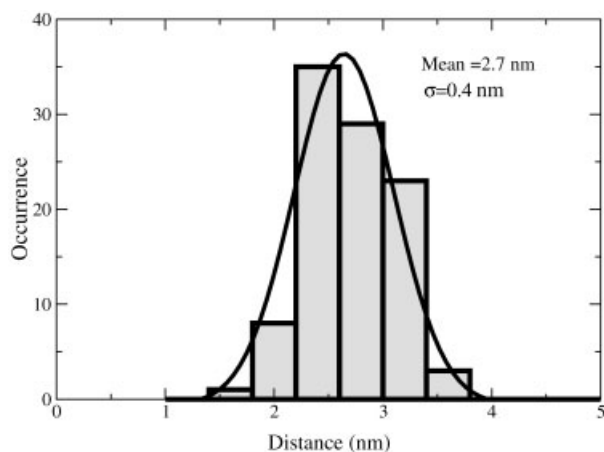
Figure 1. Distribution of the metal-to-metal distance, for the first 100 complexes sorted by the docking procedure. The continuous line gives a fit to a Gaussian curve; the corresponding mean and standard deviation values are reported.

the two metal ions, Fe and Cu in C551 and AZ, respectively. For the sorted 100 docking complexes, the metal-to-metal distance ranges from about 1.6–3.8 nm, and the corresponding histogram is characterized by a single mode distribution, well described by a Gaussian curve, centred at 2.7 nm with a standard deviation of 0.4 nm (see Figure 1). Accordingly, the largest part of these ET complexes (more than 80%) matches the requirement that the metal-to-metal distance is less than 3 nm, while about 10% are found with a distance within 2 nm.

A single-mode Gaussian distribution has been also found for the other analyzed quantities; the corresponding average and standard deviation values being reported in Table 1. The I-ASA, which is the area of the protein surfaces that has to be removed from contact with water in order to form the complex (Connolly, 1983), reflects the steric fit between the proteins. The I-ASA values, reported in Table 1, are in a good agreement with those usually observed for other transient complexes whose values range from 400 to 1000 Å^2 (Nooren and Thornton, 2003). At variance, higher values (1000–2000 Å^2) are commonly observed for permanent complexes, such as enzymes and their protein inhibitors, with a high degree of surface complementary; these complexes typically lasting for long times (days or more). Table 1 also reports an excess of nonpolar residues at

the protein–protein interface, in agreement with the fact that the protein–protein contact surface tends to be more hydrophobic than the rest of the protein surface and more similar to the protein interior. Indeed, the residues at the interface are responsible for the short-range hydrophobic interactions between proteins, playing a fundamental role in determining the specificity of protein–protein recognition (Sheinerman *et al.*, 2000).

Finally, new H-bonds have been found in the complex. The presence of additional H-bonds, while, on one hand, can stabilize the complex structure, on the other it could contribute to the ET efficiency (Beratan *et al.*, 1987; Beratan *et al.*, 1991).

As already mentioned, the sorted docking complexes are to be filtered to extract one or more complexes, matching at the best further properties. We have therefore implemented in our algorithm the searching of the shortest metal-to-metal distance in connection with the involvement of Val23 and Ile59 of C551 at the complex interface. The former criterion has been imposed to assure an efficient ET process (Marcus and Sutin, 1985). Actually, the application of such a criterion gives reliable results, as evidenced by the study of other ET complexes: e.g. Plastocyanin–Photosystem I and cytochrome *c*–cytochrome b5 complexes (Miyashita *et al.*, 2005; Mattila and Haltia, 2005; Myshkin *et al.*, 2005; Volkov *et al.*, 2005). The latter one guarantees that the complex matches the results from mutagenesis experiments (Cutruzzolà *et al.*, 2002).

The 23rd outcome from GRAMM has been classified as the BC; two different graphical representations of this complex being shown in Figure 2 (solvent-exposed surfaces) and Figure 3A (secondary structure). The two protein partners are arranged to overlook their hydrophobic patches with a distance between the two metal ions of 1.59 nm. The residues involved at the interface are listed in Figure 2. We found that Pro58 of C551 is located at the outer part of the docking region, consistently with the experimental evidence showing that its substitution does not affect the ET process (Cutruzzolà *et al.*, 2002).

All the other quantities evaluated for the BC are listed in the last column of Table 1. The I-ASA value of the BC is close to that found for other transient ET complex (Crowley and Ubbink, 2003). The large predominance of nonpolar amino acids at the docking interface is in agreement with the fact that the protein–protein contact is usually more hydrophobic than the solvent-exposed protein surface (Crowley and Ubbink, 2003). Three additional H-bonds

Table 1. Mean values and standard deviations derived from the extracted 100 docking structures

	Mean value (standard deviation)	Best complex
Metal-to-metal distance (nm)	2.42 (0.42)	1.59
I-ASA (Å^2)	580 (60)	657
% polar atoms at the interface	44.2 (10.1)	25.7
% nonpolar atoms at the interface	54.0 (10.0)	74.3
Number of H-bonds	3.7 (1.7)	5

The last column shows the values related to the best complex. The I-ASA has been evaluated by rolling a probe sphere of radius 1.4 Å over its surface by using the protein–protein Interaction Server (http://www.biochem.ucl.ac.uk/bsm/PP/server/). A H-bond is formed when the distance between a hydrogen with a compatible donor atom is in a range of 1.2–2.76 Å (Guex and Peitsch, 1997).
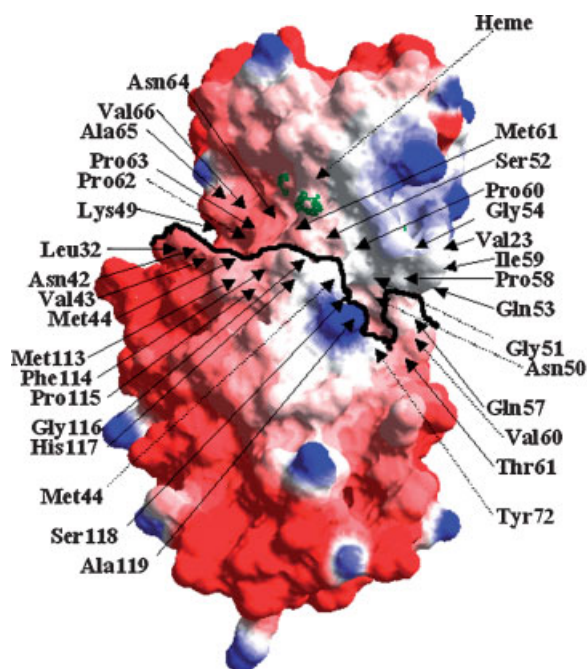
Figure 2. The solvent-accessible-surface of the structure of the BC as obtained by docking between AZ and C551. Black line indicates the monomer–monomer interface of the complex. The surface is coloured according to the residue hydrophobicity: blue, hydrophilic; red, hydrophobic; white, intermediate. The heme is marked by a green line. The list of residues involved at the protein–protein interface is also reported.
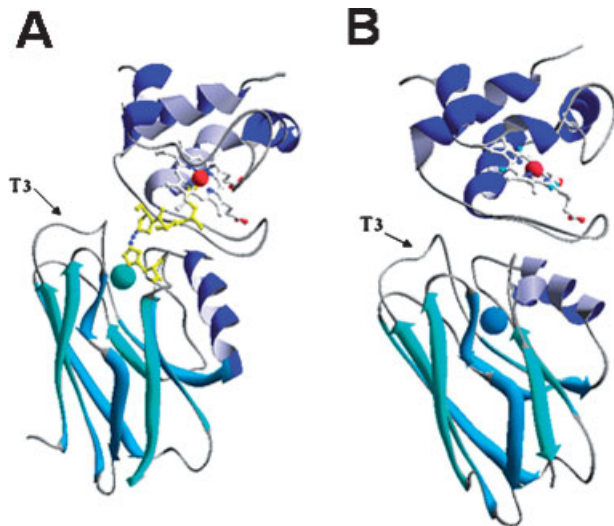

Figure 3. A: Molecular graphic representation of the BC. Yellow ball-and-sticks (covalent bonds) and blue dotted lines (free space jumps) show the ET path between the AZ copper and C551 iron atoms. B: Molecular graphic representation of the complex as obtained by averaging the structures from the 10–60 MD simulation trajectory. The copper (blue sphere) and the iron (red sphere) are also shown.

are formed in the BC with respect to free proteins: between Pro63 of C551 and Pro115 of AZ, Gln 33 of C551 and Glu 57 of AZ and Gln53 of C551 and Met64 of AZ. The occurrence of these new H-bonds could contribute to the stability of the BC.

The geometrical configuration of the BC has been taken into account to plan atomic force spectroscopy experiments aimed at measuring the interaction forces between AZ and C551 (Bonanni *et al.*, 2005). In particular, AZ was bound to a gold substrate through its native disulphide group, opposite to the interaction region, with its hydrophobic patch oriented towards the AFM tip. Conversely, C551 was linked to the tip by means of a few-nm-long linker allowing protein reorientation, thus facilitating mutual interaction. In this way, we detected multiple specific molecular recognition events between the two partners with an unbinding force of (95 ± 15) pN and a k_{off} rate of $(14 \pm 2)\,\text{s}^{-1}$ (Bonanni *et al.*, 2005).

ET properties of the best complex

The ET properties of the BC can be evaluated by applying the empirical Pathways model (Beratan *et al.*, 1987; Beratan *et al.*, 1991). From the classical Marcus theory, the ET reaction rate between D and A, in the weak coupling limit, is given by (Marcus and Sutin, 1985)

$$k_{\text{ET}} = \frac{1}{\hbar} V_{\text{R}}^2 \left(\frac{\pi}{\lambda k_{\text{B}} T} \right)^{1/2} e^{-\frac{(\Delta G^{\circ} + \lambda)^2}{4\pi \lambda k_{\text{B}} T}} \quad (1)$$

where V_{R} is the electronic tunnelling matrix element between D and A, λ is the reorganization energy and ΔG^{o} is the driving force of the reaction. The dependence of k_{ET} on the medium between the redox centres is mainly reflected by V_{R} which can be cast in the form: $V_{\text{R}}^2 = V_{\text{R}}^{o2} f_{\text{M}}^2$, where V_{R}^o represents the electronic coupling between the redox centres in van der Waals contact, and f_{M} is a dimensionless attenuation factor directly taking into account the dependence of the ET process on the medium. In the framework of the Pathways model, for which the ET path is a combination of three types of steps between atoms (covalent bond (C), hydrogen bond (H) and through free space (S); Beratan *et al.*, 1987), f_{M} can be expressed as:

$$f_{\text{M}} = \prod_i^{N_{\text{C}}} \varepsilon_i^{\text{C}} \prod_j^{N_{\text{H}}} \varepsilon_j^{\text{H}} \prod_k^{N_{\text{S}}} \varepsilon_k^{\text{S}} \quad (2)$$

where N_{C}, N_{H} and N_{S} are the number of C, H and S paths, respectively; ε_i being the corresponding attenuation factors. Semiempirical expressions for the ε-factors are (Beratan *et al.*, 1991)

$$\varepsilon^{\text{C}} = 0.6; \quad \varepsilon^{\text{H}} = 0.36 e^{[-17(R - 0.28)]}; \quad \varepsilon^{\text{S}} = 0.6 e^{[-17(R - 0.14)]} \quad (3)$$

where R is the distance between D and A. The best pathway from Fe of C551 to Cu of AZ has been extracted by evaluating, among all the possible paths through C-H-S steps, the path that maximizes the f_{M} term and, in turn, the electronic coupling (Kurnikov, 2004). The resulting ET pathway starts from the Fe ion, then involves 14 covalent bonds through Met61, Pro62 and Pro63 of C551, and a free jump to His117 of AZ and finally ends at the copper ion (see Figure 3A). The fact that Hys117 is involved in the ET path
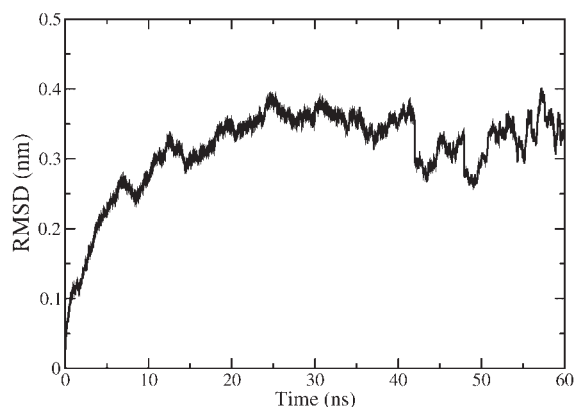
Figure 4. RMSD calculated by $< (r_i^A - r_j^B)^2 >^{1/2}$ from the starting structure of the AZ-C551 along a 60 ns trajectory. The RMSD have been obtained by averaging over all the protein atoms.

Figure 5. The RMSF, calculated by $< (r_i - < r_i >)^2 >^{1/2}$, of the backbone atoms plotted versus residue number, of the complex (continuous line), of a single AZ molecule (black, dashed line, residue number 1–128) and of a single C551 molecule (grey, dashed line, residue number 128–210). The residue numbers corresponding to the protein–protein interface are marked as black boxes. In all the cases, the RMSF were obtained by averaging over the 10–60 ns MD trajectory. The RMSF averaged over the all atoms are: (0.110 ± 0.038) nm for the AZ–C551 complex, (0.079 ± 0.031) nm for AZ and (0.089 ± 0.027) nm for C551.

agrees with the experimental results obtained *in vitro* (Cutruzzolà *et al.*, 2002). The corresponding square electronic tunnelling matrix V_R^2 has been estimated to be 2.8×10^{-7}, indicating a good electronic coupling between D and A. Furthermore, upon calculated V_R^2, an estimation of the maximum ET rate can be obtained under the assumption of an activationless process ($\Delta G^\circ = -\lambda$). Actually, Equation 1, assumes the form $k_{ET} \sim A\, V_R^2$, where the prefactor A, including the Franck–Condon term, and ranges between 10^{14}–$10^{16}\,s^{-1}$ (Page *et al.*, 1999; Miyashita *et al.*, 2005). By fixing $A = 10^{14}\,s^{-1}$, a value commonly used in the theoretical works (Tan *et al.*, 2004; Miyashita *et al.*, 2005), we found a maximum ET rate of $2.8 \times 10^7\,s^{-1}$.

MD simulation of the best complex

A 60 ns classical MD simulation of the BC has been carried out at full hydration to investigate the dynamical behaviour of the two proteins upon forming the complex. The Root Mean Square Displacement (RMSD) of all atoms from the starting structure is shown in Figure 4. At first, it undergoes an initial rising, lasting about 1.5 ns, commonly attributed to a breakdown from the crystallographic structure (Levitt and Sharon, 1988). Then, the RMSD reaches an average value of 0.3 nm, around which rather slow, marked oscillations take place. Such a trend suggests that the MD simulation of the complex is substantially stable, even if some structural reassessments might continuously occur during the run. We also note that the RMSD average value is higher than that observed for the single AZ and C551 proteins (Arcangeli *et al.*, 1999; Ceruso *et al.*, 2003).

To get a closer insight into these structural changes, we have compared the structure of the complex, obtained by averaging the trajectory over the last 50 ns, with the initial configuration as extracted from the docking procedure (see Figure 3A and 3B). It comes out that the overall orientation of the two proteins is preserved even if slight changes in the orientation of the heme group of C551 and in the large T3 turn of AZ, located just at the outer region of the interface area can be registered. Furthermore, the I-ASA of the average BC structure slightly increases from 657 to 680 Å²,
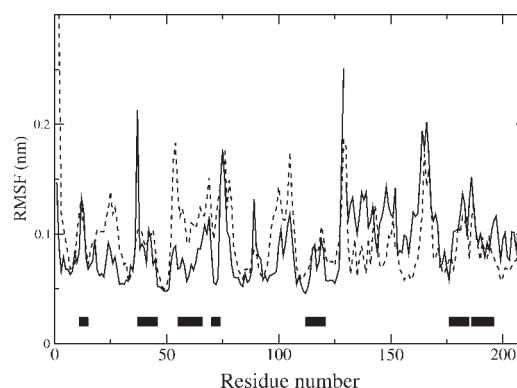
consistently with a better surface matching, likely promoted by the presence of hydration water (Pal and Zewail, 2004). Such a behaviour is also coupled to a change in the BC flexibility, as investigated by the Root Mean Square Fluctuations (RMSF), and shown in Figure 5 as a function of the residue number. For comparison, the RMSF of the isolated AZ and C551 proteins have also been shown. The RMSF of the BC appears higher than those of the isolated proteins in most of the interface residues, e.g. 51–55 residues of AZ (see also the averaged RMSF values in the legend of Figure 5). Such an effect can be put in relationship to the hydrophobic character of the involved residues, whose dynamics is restricted in the presence of a polar medium (aqueous solvent), while it can be enhanced in the hydrophobic environment, as observed in other systems (Myshkin *et al.*, 2005).

We have also analyzed the temporal evolution of the metal-to-metal distance. Such a distance reaches an almost stable value of about 1.6 nm, after 7 ns (see Figure 6). Around this value, fast amplitude fluctuations (of about 0.15 nm) are observed in the temporal scale of picoseconds. Moreover, at almost regular time intervals of about 15 ns, rapid jumps, up to about 2 nm, take place (see the arrows in Figure 6); these higher values being observed for time intervals ranging from 0.5 to 1.5 ns. Such a behaviour is reminiscent of a bimodal trend and it can be generally attributed to a nonlinear dynamics (Krumhansl, 1987). Furthermore, it resembles that observed for their dynamical quantities of proteins in different time windows (Garcia, 1992; Bizzarri and Cannistraro, 1998; Carlini *et al.*, 2002). These nonlinear phenomena could be traced back to the sampling of the local minima (conformational substates), organized in a hierarchical way, in the potential energy hypersurface of the protein macromolecules (Garcia *et al.*, 1997; Carlini *et al.*, 2002). Actually, transitions among these states, driven by collective, anharmonic motions of the
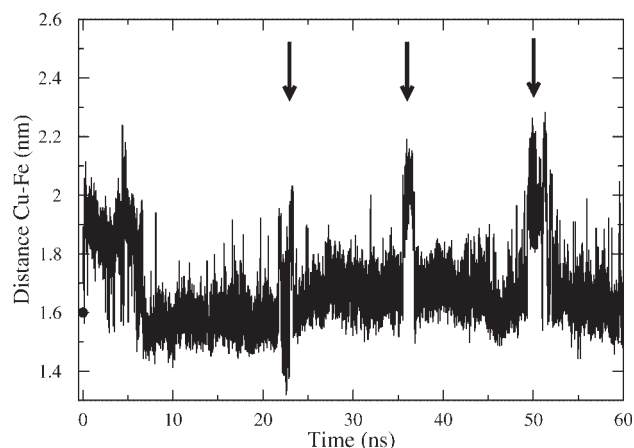
Figure 6. Temporal evolution of the metal-to-metal distance, during the MD simulation run of the complex. Arrows indicate the times at which rapid jumps are detected during the dynamics. The initial value is marked as a circle.

Figure 7. Occurrence of the residues participating to the ET paths of 500 structures of the complex, sampled every 0.1 ns of the 10–60-ns MD trajectory of the complex; only residues with an occurrence exceeding 15% being shown. AZ is marked as dark boxes and C551 as dashed boxes.

polypeptide chain, might be associated to some biological functionality (Frauenfelder *et al.*, 1988).

The observed bimodal trend of the metal-to-metal distance has led us to speculate about the possibility that it could have some relevance for the ET process. Indeed, the time that the system spends in the configuration with the shortest metal-to-metal distance (about 15 ns), finds a good correspondence with the characteristic time τ of the ET process in our system, $\tau = 1/k_{ET}^{max} \sim 30$ ns. Accordingly, the system might switch from an ET-favourable to a less ET-favourable, or unfavourable, configuration; the ET process occurs during the favourable configuration.

In this connection, it is interesting to analyze the evolution of the ET properties during the simulated dynamical evolution. We have therefore monitored the ET path and the electronic tunnelling matrix, by sampling the structures of the complex every 0.1 ns during the last 50 ns of the MD run. We have found that rather small values for the square electronic tunnelling matrix element (less than 10^{-10}) when the metal-to metal distance is around 2 nm. At smaller d_{Fe-Cu} values, the electronic tunnelling matrix, increases up to 10^{-6}, with an average value of 3×10^{-8}. The most efficient ET process is observed at 11.2 ns at which an electronic tunnelling matrix of 6×10^{-6} and a maximum ET rate of $6 \times 10^{8}\,s^{-1}$ have been observed. These results are consistent with the fact that, during the dynamics, the complex explores a variety of configurations to which different ET rates might correspond (Daizadeh *et al.*, 1997; Yang *et al.*, 2003).

During the MD, we have observed that the ET takes place through different paths involving different residues; a histogram related to the occurrence of the most frequent residues participating in the ET process is shown in Figure 7. Notably, both His117 of AZ and Met61 of C551 have a frequency percentage higher than 50%, confirming a predominant role played by these residues in controlling the ET process, in agreement with the experiments. Furthermore, some ET paths involve a single water molecule acting as a bridge between AZ and C551, through H-bonds. Interestingly, the same water molecule has been often
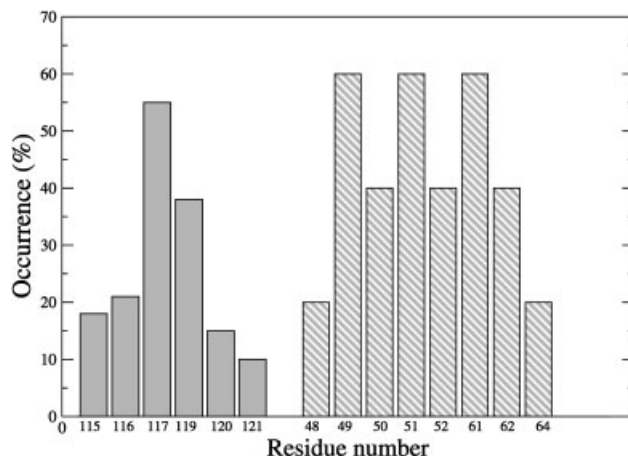
observed to persist in successive ET paths; such a behaviour supporting the hypothesis that structured water is favourite in water-mediated intermolecular ET paths, has been suggested by Lin *et al.* (2005).

Figure 8 shows the I-ASA of the complex as a function of simulation time. It ranges from about 580 to 690 Å^2 with an average of about 640 Å^2, a value close to the initial one. These results indicate that no drastic changes occur at the protein–protein interface, consistently with the preservation of the overall complex structure in the analyzed temporal window. The temporal trend shows slow fluctuations on a temporal scale of nanosecond, on which fast fluctuations in the picosecond time scale are overimposed. A cross-correlation analysis (see the legend of Figure 8) has revealed that there is no correlation between the I-ASA and the Fe–Cu distance fluctuations. In other words, the observed jumps in the metal-to-metal distance do not find a correspondence in the I-ASA trend.
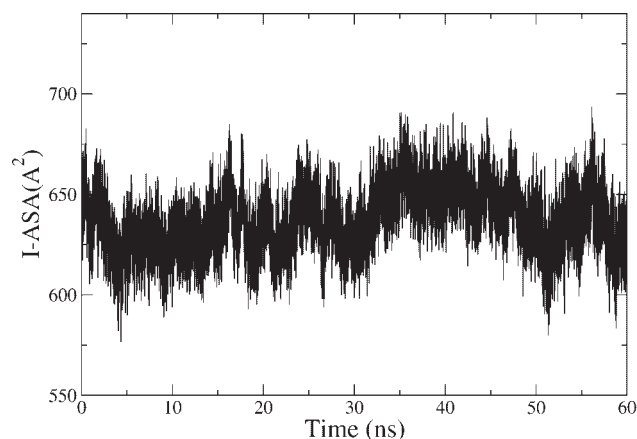

Figure 8. Temporal evolution of the I-ASA during the MD simulation run of the complex. The cross-correlation, calculated at delay time zero, between the temporal trend of the Fe–Cu distance (see Figure 6) and of the I-ASA gives a value 0.1, indicating there is no correlation between the two quantities.
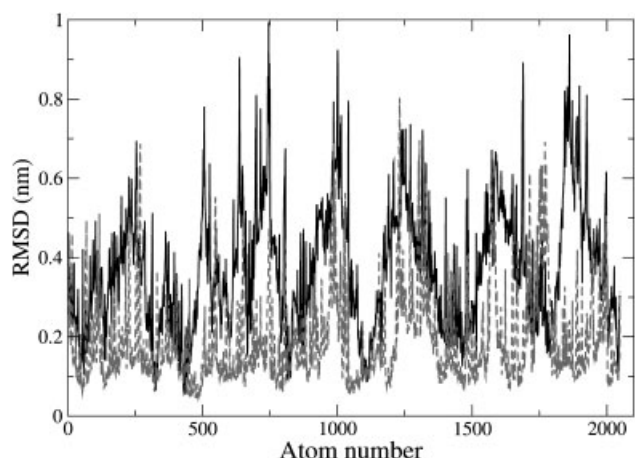
Figure 9. The RMSD as a function of the jump around 37 ns of the MD run from the structure of the complex before the jump, plotted versus the atom number (continuous black curve) for a time interval of 0.5 ns. The RMSD as obtained for a time interval of 0.5 ns around 15 ns (dashed grey curve) where no jumps in the metal-to-metal distance have been observed.

We wonder, therefore, if the complex switches to different structures when a sudden rise in the metal-to-metal distance takes place. A visual inspection of the MD snapshots before and immediately after each jump does not reveal any global structural change. It appears that both the orientation and the relative arrangement of the two molecules are substantially preserved for all the three cases (not shown). We cannot, however, rule out the possibility that some local changes could take place. To investigate such an aspect, we have analyzed the RMSD from the structure of a complex before the jump, as a function of the atom number. We found that the RMSD curves are rather similar for the three jumps; an example being shown in Figure 9. It turns out that the RMSDs as calculated in relation to a jump (continuous black curve) are slightly higher if compared with the RMSDs obtained from a time interval of the run without any jump (dashed grey curve).

These results are indicative that the observed jumps in the metal-to-metal distance might arise from a superposition of many local changes, which, however, do not result into a different global arrangement for the complex. It can then be speculated about the occurrence of a fine tuning of the dynamical properties of the protein to control its ET properties. Such an aspect is particularly intriguing and deserves further investigation even in other ET complexes.

CONCLUSIONS

The application of a docking strategy procedure has allowed us to figure out a recognition complex between AZ and C551 whose transient character makes difficult an experimental investigation. The results show that the sorted best complex is characterized by a short distance between the metal ions in the two redox sites and by a close contact between the hydrophobic regions of both proteins. In this configuration, the ET properties, as evaluated by the Pathways model, appears to be in good agreement with the experimental data. MD simulation carried out on the fully hydrated best complex, has revealed that the two proteins substantially maintain their relative spatial positions for 60 ns; while some changes in the ET properties are observed. Very interestingly, the metal-to-metal distance is shown to undergo a peculiar bimodal trend with time, which is reminiscent of a nonlinear dynamics and whose possible connection with the ET process deserves further investigation. Finally, we remark that a combined use of MD simulation and docking procedures, appears to be very promising in the study of ET complexes to get insight into the coupling among the structure, dynamics and functionality.

Acknowledgments

REFERENCES

Andolfi L, Cannistraro S. 2005. Conductive atomic force microscopy study of plastocyanin adsorbed on gold electrode. *Surf. Science* **598**: 68–77.

Arcangeli C, Bizzarri AR, Cannistraro S. 1999. Long-term molecular dynamics simulation of copper azurin: structure, dynamics and functionality. *Biophys. Chem.* **78**: 247–257.

Bendall DS. 1996. Interprotein electron transfer. In Protein Electron Transfer, Bendall DS (ed.). Bios Scientific: Oxford; 43–64.

Beratan DN, Onuchic JN, Hopfield JJ. 1987. Electron tunnelling through covalent and noncovalent pathways in proteins. *J. Chem. Phys.* **86**: 4488–4498.

Beratan DN, Betts JN, Onuchic JN. 1991. Protein electron transfer rates set by the bridging secondary and tertiary structure. *Science* **252**: 1285–1288.

Berendsen HJC, van der Spoel D, van Drunen R. 1995. GROMACS: a message-passing parallel molecular dynamics implementation. *Comp. Phys. Comm.* **91**: 43–56.

Berendsen HJC, Grigera JR, Straatsma TP. 1997. The missing term in effective pair potentials. *J. Phys. Chem.* **91**: 6269–6271.

Bizzarri AR, Cannistraro S. 1998. Molecular dynamics simulation of plastocyanin potential energy fluctuations: 1/f noise. *Phys. Letters A.* **267**: 257–270.

Bizzarri AR, Cannistraro S. 2005. Electron transfer in metalloproteins. In Encyclopedia of Condensed Matter Physics, Bassani G (ed.). Elsevier: Amsterdam; 361–369.

Bizzarri AR, Andolfi L, Stchakosky M, Cannistraro S. 2005. AFM, STM, and ellipsometry characterization of a monolayer of Azurin molecules self-assembled on a gold surface in air. *J. Nanotechnology* **A0100**: 1–11.

Bonanni B, Kamruzzahan ASM, Bizzarri AR, Rankl C, Gruber HJ, Hinterdorfer P, Cannistraro S. 2005. Single molecule recognition between cytochrome C 551 and gold-immobilized Azurin by force spectroscopy. *Biophys. J.* **89**: 2783–2791.

Bonanni B, Bizzarri AR, Cannistraro S. 2006. Optimized biore-congnition of cytochrome C 551 and Azurin on thiol-terminated monolayers assembled on Au(111) substrates. *J. Phys. Chem. B.* **110**: 14574–14580.

Carlini P, Bizzarri AR, Cannistraro S. 2002. Temporal fluctuations in the potential energy of proteins: $1/f^\alpha$ noise and diffusion. *Phys. D.* **165**: 242–250.

Ceruso MA, Grottesi A, Di Nola A. 2003. Dynamics effects of mutations within two loops of cytochrome C551 from Pseu-domionas aeruginosa. *Proteins* **50**: 222–229.

Chothia C, Janin J. 1975. Principles of protein-protein recog-nition. *Nature* **256**: 705–708.

Connolly ML. 1983. Solvent-accessible surfaces of proteins and nucleic acids. *Science* **221**: 709–713.

Crowley PB, Ubbink M. 2003. Close encounters of the transient kind: protein interactions in the photosynthetic redox chain investigated by NMR spectroscopy. *Acc. Chem. Res.* **36**: 723–730.

Cutruzzolà F, Arese M, Ranghino G, van Pouderoyen G, Canters GW, Brunori M. 2002. *Pseudomonas aeruginosa* cytochrome C551: probing the role of the hydrophobic patch in electron transfer. *J. Inorg. Biochem.* **88**: 353–361.

Daizadeh I, Medvedev ES, Stuchebrukhov AA. 1997. Effect of protein dynamics on biological electron transfer. *Proc. Natl. Acad. Sci. USA* **94**: 3703–3708.

Darden T, York D, Pedersen L. 1993. Particle mesh Ewald: an N_log (N) method for Ewald sums in large systems. *J. Chem. Phys.* **98**: 10089–10092.

Farver O, Lu Y, Ang MC, Pecht I. 1999. Enhanced rate of intra-molecular electron transfer in an engineered purple CuA azurin. *Proc. Natl. Acad. Sci. USA* **96**: 899–902.

Frauenfelder H, Parak F, Young RD. 1988. Conformational sub-states in proteins. *Ann. Rev. Biophys. Biophys. Chem.* **17**: 451–479.

Gabdoulline RR, Wade RC. 2001. Protein-protein association: investigation of factors influencing association rates by Brownian dynamics simulations. *J. Mol. Biol.* **306**: 1139–1155.

Garcia AE. 1992. Large amplitude nonlinear motions in proteins. *Phys. Rev. Lett.* **68**: 2696–2699.

Garcia AE, Blumenfeld R, Hummer G, Krumhansl JA. 1997. Multi-basin dynamics of a protein in a crystal environment. *Phys. D.* **107**: 225–239.

Gray HB, Winkler JR. 1996. Electron transfer in proteins. *Ann. Rev. Biochem.* **65**: 537–561.

Guex N, Peitsch MC. 1997. SWISS-MODEL and the Swiss-PdbViewer: an environment for comparative protein modeling. *Electrophoresis* **18**: 2714–2723.

Guzzi R, Bizzarri AR, Sportelli L, Cannistraro S. 1997. An EPR investigation on the structural heterogeneity in copper azurin and plastocyanin. *Biophys. Chem.* **63**: 211–219.

Hess B, Bekker H, Berendsen HJC, Fraaije JGEM. 1996. LINCS: a linear constraint solver for molecular simulations. *J. Comp. Chem.* **18**: 1463–1472.

Janin J, Rodier F. 1995. Protein-protein interaction at crystal contacts. *Proteins* **23**: 580–587.

Jiang S, Tovchigrechko A, Vakser IA. 2003. The role of geometric complementarity in secondary structure packing: a systema-tic docking study. *Protein. Sci.* **12**: 1646–1651.

Jones S, Thornton JM. 1996. Principles of protein-protein inter-actions. *Proc. Natl. Acad. Sci. USA* **93**: 13–20.

Katchalski-Katzir E, Shariv I, Eisenstein M, Friesem AA, Aflalo C, Vakser IA. 1992. Molecular surface recognition: determi-nation of geometric fit between proteins and their ligands by correlation techniques. *Proc. Natl. Acad. Sci. USA* **89**: 2195–2199.

Kholmurodov K, Smith W, Yasuoka K, Darden T, Ebisuzaki T. 2000. A smooth-particle mesh Ewald method for DL_POLY molecular dynamics simulation package on the Fujitsu VPP700. *J. Comput. Chem.* **21**: 1187–1191.

Krumhansl JA. 1987. Anharmonicity and Debye-Waller factors in biomolecules. In *Proceedings in Life Science: Protein Struc-ture, Molecular and Electronic Reactivity*, Austin RH (ed.). Springer-Verlag: New York; pp 50–57.

Kurnikov IV. 2004. *HARLEM: Biomolecular modeling packa-ge* http://www.kurnikov.org/harlem

Levitt M, Sharon R. 1988. Accurate simulation of protein dynamics in solution. *Proc. Natl. Acad. Sci. USA* **85**: 7557–7561.

Liang ZX, Kurnikov IV, Nocek JM, Mauk AG, Beratan DN, Hoff-man BM. 2004. Dynamic docking and electron-transfer between cytochrome *b*5 and a suite of myoglobin surface-charge mutants: introduction of a functional-docking algor-ithm for protein–protein complexes. *J. Am. Chem. Soc.* **126**: 2785–2798.

Lin J, Balabin IA, Beratan DN. 2005. The Nature of aqueous tunneling pathways between electron-transfer. *Science* **310**: 1311–1313.

Lindahl E, Hess B, van der Spoel D. 2001. GROMACS 3.0: a package for molecular simulation and trajectory analysis. *J. Mol. Model.* **7**: 306–317.

Marcus RA, Sutin N. 1985. Electron transfers in chemistry and biology. *Biochim. Biophys. Acta.* **811**: 265–322.

Marvin JS, Hellinga HW. 2001. Conversion of a maltose receptor into a zinc biosensor by computational design. *Proc. Natl. Acad. Sci. USA* **98**: 4955–4960.

Mathews FS, Mauk AG, Moore GR. 2000. Protein-protein com-plexes formed by electron-transfer proteins. In Protein-Protein Recognition, Kleanthous C (ed.). Oxford University Press: New York; pp 60–101.

Matsuura Y, Takano T, Dickerson RE. 1982. Structure of cyto-chrome c551 from *P. aeruginosa* refined at 1.6 angstroms resolution and comparison of the two redox forms. *J. Mol. Biol.* **156**: 389.

Mattila K, Haltia T. 2005. How does nitrous oxide reductase interact with its electron donors? A docking study. *Proteins* **59**: 708–721.

Miyashita O, Okamura Y, Onuchic JN. 2005. Interprotein electron transfer from cytochrome c2 to photosynthetic reaction center: tunneling across an aqueous interface. *Proc. Natl. Acad. Sci. USA* **102**: 3558–3563.

Moser CC, Keske JM, Warncke K, Farid RS, Dutton PL. 1992. Nature of biological electron transfer. *Nature* **366**: 796–802.

Myshkin E, Leontis NB, Bullerjahn GS. 2005. Computational simulation of the docking of *Prochlorothrix hollandica* plas-tocyanin to photosystem I: modeling the electron transfer complex. *Biophys. J.* **82**: 3305–3313.

Nar H, Messerschmidt A, Huber R, van de Kamp M, Canters GW. 1991. Crystal structure analysis of oxidized *Pseudomonas Aeruginosa* azurin at pH 5.5 and pH 9.0. a pH-induced con-formational transition involves a peptide bond flip. *J. Mol. Biol.* **221**: 765–772.

Nooren IMA, Thornton JM. 2003. Structural characterization and functional significance of transient protein-protein inter-actions. *J. Mol. Biol.* **325**: 991–1018.

Northrup SH, Erickson HP. 1992. Kinetics of protein-protein association explained by Brownian dynamics computer simulation. *Proc. Natl. Acad. Sci. USA* **89**: 3338–3342.

Nosé S. 1984. A molecular dynamics method for simulations in the canonical ensemble. *Mol. Phys.* **52**: 255–268.

Paciaroni A, Stroppolo ME, Arcangeli C, Bizzarri AR, Desideri A, Cannistraro S. 1999. Incoherent neutron scattering of copper azurin: a comparison with molecular dynamics simulation results. *Eur. Biophys. J.* **28**: 447–456.

Page CC, Moser CC, Chen X, Dutton PL. 1999. Natural engineer-ing principles of electron tunneling in biological oxidation-reduction. *Nature* **402**: 47–52.

Pal SK, Zewail AK. 2004. Dynamics of water in biological recog-nition. *Chem. Rev.* **104**: 2099–2123.

Prudêncio M, Ubbink M. 2004. Transient complexes of redox proteins: structural and dynamics from NMR studies. *J. Mol. Recogn.* **17**: 524–539.

Sheinerman FB, Norel R, Honig B. 2000. Electrostatic aspects of protein-protein interactions. *Curr. Opin. Struct. Biol.* **10**: 153–159.

Silvestrini MC, Tordi MG, Colosimo A, Antonini E, Brunori M. 1982. The kinetics of electron transfer between *Pseudomo-*

nas *Aeruginosa* cytochrome *c*-551 and its oxidase. *Biochem. J.* **203**: 445–451.

Smith GR, Sternberg MJE. 2002. Prediction of protein–protein interactions by docking methods. *Curr. Opin. Struct. Biol.* **12**: 28–35.

Solomon EI, Baldwin MJ, Lowery MD. 1992. Electronic structures of active sites in copper proteins: contributions to reactivity. *Chem. Rev.* **92**: 521–542.

Swart M. 2002. *Density functional theory applied to copper proteins*. PhD Thesis. Groningen, Rijksuniversiteit Groningen.

Tan ML, Balabin I, Onuchic JN. 2004. Dynamics of electron transfer pathways in cytochrome c oxidase. *Biophys. J.* **86**: 1813–1819.

Tovchigrechko A, Wells CA, Vakser IA. 2002. Docking of protein models. *Protein. Sci.* **11**: 1888–1896.

Ullmann GM, Knapp EW, Kostíc NM. 1997. Computational simulation and analysis of dynamic association between plastocyanin and cytochrome f. consequence for the electron-transfer reaction. *J. Am. Chem. Soc.* **119**: 42–52.

Vajda S, Camacho CJ. 2004. Protein-protein docking: is the glass half-full or half-empty? *Trends Biotechnol.* **22**: 110–116.

Vakser IA, Aflalo C. 1994. Hydrophobic docking : a proposed enhancement to molecular recognition techniques. *Proteins* **20**: 320–329.

Vakser IA, Matar OG, Lam CF. 1999. A systematic study of low-resolution recognition in protein-protein complexes. *Proc. Natl. Acad. Sci. USA* **84**: 77–8482.

van de Kamp M, Silvestrini MC, Brunori M, Beeumen JV, Hali FC, Canters GW. 1990. Involvement of the hydrophobic patch of azurin in the electron-transfer reactions with cytochrome c551 and nitrite reductase. *Eur. J. Biochem.* **194**: 109–118.

van Gunsteren WF, Billeter SR, Eising AA, Huenenberger PH, Krueger P, Mark AE, Scott WRP, Tironi IG. 1996. *Biomolecular simulation: GROMOS96 manual and user guide; BIOMOS: Zurich, Groningen*.

Volkov AN, Ferrari D, Worrall JAR, Bonvin AMJJ, Ubbink M. 2005. The orientations of cytochrome *c* in the highly dynamic complex with cytochrome b_5 visualized by NMR and docking using HADDOCK. *Protein Sci.* **14**: 799–811.

Webb MA, Loppnow GR. 1999. A structural basis for long-range coupling in Azurins from resonance raman spectroscopy. *J. Phys. Chem. A.* **103**: 6283–6287.

Willner I, Katz E. 2000. Integration of layered redox proteins and conductive supports for bioelectronic applications. *Angew. Chem. Int. Ed.* **39**: 1180–1218.

Yang H, Luo G, Karnchanaphanurach P, Louie TM, Rech I, Cova S, Xun L, Xie XS. 2003. Protein conformational dynamics probed by single-molecule electron transfer. *Science* **302**: 262–266.